EARTHQUAKE ARCHAEOLOGY

PALEOSEISMOLOGICAL INVESTIGATIONS IN THE NORTHERN TIEN SHAN NEAR BISHKEK (KYRGYZSTAN)

Landgraf, A. (1), Abdrakhmatov, K.. (2), Djumabaeva, A. (2), Strecker, M.R. (1), Arrowsmith, J.R. (3)

(1) Inst. Für Erd- und Umweltwissenschaften, Universität Potsdam, Potsdam, GERMANY. landgraf@geo.uni-potsdam.de
(2) Kyrgyz Institute of Seismology, Bishkek, KYRGYZSTAN.
(3) School of Earth and Space Exploration, Arizona State University,Tempe, USA

***Abstract**: The northern Tien Shan was affected by a series of major earthquakes in the late 19th and earliest 20th centuries, which are amongst the largest known intraplate earthquakes worldwide: 1885 (Ms 6.9), 1887 (Ms 7.3), 1889 (Ms 8.3), and 1911 (Ms 8.1). We started paleoseismological investigations near Panfilovkoe, about 75 km west of the Kyrgyz capital Bishkek, where youthful scarps in alluvial-fan deposits attest to sub-recent ground deformation. The alluvial fan has been active since Late Pleistocene time and comprises distinguished lobes with vertical offsets between about 0.6 m and 3.8 m, respectively. Three trenches, excavated in the main scarp, have revealed that this offset distribution reflects repeated surface rupturing earthquakes with predominant dip-slip motion. The ultimate event was characterized by an offset between 1.2 and 1.4 m, corresponding to a possible magnitude between 6.8 and 7.2, emphasizing the seismogenic nature of the Tien Shan with infrequent, large magnitude earthquakes.*

***Key words**: Intracontinental paleoearthquakes, Tien Shan, Kyrgyzstan*

Introduction

The Kyrgyz Tien Shan is an intracontinental orogen, characterized by reverse-fault bounded ranges, ubiquitous evidence for active tectonism and mainly moderate earthquake magnitudes (Kalmetieva et al., 2009). Although about 22 mm/a of shortening, which constitutes about half of the total convergence between India and Eurasia, are accommodated in the Tien Shan (Zubovich et al., 2010), Quaternary deformation phenomena, including decadal time scales, show that this rate is widely distributed across the entire belt, leading to slip rates of 1-2 mm/a for individual faults (Thompson et al., 2002; Zubovich et al., 2010). The historic earthquake in Kyrgyzstan (Fig. 1) reaches back to 250+/-100 yrs BP (e.g., Abdrakhmatov et al., 2002; Kalmetieva et al., 2009). From reported damage, magnitudes > 6 have been inferred for many of these events. However, such reports are often incomplete and biased for instance by the population distribution as well as cultural or political transitions, accompanied by widespread destruction and loss of documentation. The location of the Tien Shan and present-day Kyrgyzstan between the northern and southern branches of the silk route (e.g., Korjenkov et al., 2003) might have resulted in higher population density along the former trade routes and thus a higher probability that earthquakes affecting these areas got reported. Indeed, the distribution of significant events (M > 6.5) seems to be concentrated along the northern and southern sectors of the Tien Shan, respectively (Fig. 1). At the turn of the 19th century, a series of large-magnitude earthquakes, exceeding magnitude 7, affected the northern Tien Shan in 1885 (Ms 6.9), 1887 (Ms 7.3), 1889 (Ms 8.3), and 1911 (Ms 8.1) (e.g., Abdrakhmatov et al., 2002). This corresponds to a large amount of energy released in such a short period of time in an intraplate setting. Furthermore, the epicentral areas of these events were located near the present-day Kyrgyz capital (Bishkek) and the previous Kazakh capital Almaty (formerly Alma-Ata or Verny), which were severely damaged.

The spatiotemporal clustering of these events might show a synchronization of the associated faults (e.g., Scholz, 2010), possibly promoting fault (segment)-wise triggering or alternating of subsequent shocks or events, as observed in other areas such as along the Denali fault (Eberhart-Phillips et al., 2003), the North Anatolian fault (Stein et al., 1997; Hubert Ferrari et al., 2000), or along the eastern Californian shearzone (Rockwell et al., 2000).
For a better mechanistic understanding of these events it is crucial to document the exact historic rupture patterns, to increase the time span of observation concerning previous events along the ruptured fault systems, and to analyze their paleo-seismic history. This will help to better understand, if the observed seismic behavior is unique or recurrent, and if any kind of pattern can be distinguished from these records. In this study, we have started paleo-seismological investigations near Bishkek, Kyrgyzstan, in the vicinity of the 1885 event epicentral area.

Paleo-earthquakes at Panfilovkoe

The study area is located north of the Kyrgyz range, thus along the northern margin of the Tien Shan (Fig. 1). The main structures that bound the Kyrgyz range to the north, are the en échelon arranged Chonkurchak and Shamsi-Tunduk faults (e.g., Thompson et al., 2002). The Chonkurchak fault marks the boundary between pre-Cenozoic basement and late Cenozoic deposits at the western range front. In the central part of the Kyrgyz range, where the deformation front has migrated northwards, Neogene sediments are thrusted over foreland deposits along the approximately 120 km long Issyk-Ata fault, a splay of the Chonkurchak and Shamsi-Tunduk fault system. Thompson et al. (2002) have estimated a Quaternary slip rate of 2.1 +1.7/-0.3 mm/yr for its central part.
We present paleoseismic data from a site, located about 35 km west of Belovodskoie, the epicenter of the 1885 (Ms 6.9) earthquake, about 75 km west of Bishkek in the immediate foreland of the Kyrgyz range. The site

(Panfilovkoie) is comprises youthful, north-facing scarps, probably related to activity of the Chonkurchak fault. The scarps cut through an alluvial fan, whose former transport surface is inclined about 3-4° to the north; this surface is nested inside a late Pleistocene loess terrace (Fig. 2). The northern, more prominent and approximately E-W striking scarp can be followed for about 4 km across the alluvial fan. This scarp is aligned with a cumulative break in topography of about 13 m in the loess-covered surface to the west. The trace of the scarp suggests a dominant reverse-faulting mechanism. The subordinate southern scarp trends ENE-WSW and mainly comprises left-stepping segments, suggesting a minor left-lateral component of motion due to oblique shortening. The alluvial fan is composed of different lobes of boulder-rich alluvial deposits with distinct offsets between about 0.6 m and 3.8 m. Three trenches (PT1 to PT3, marked as stars in Fig. 2) were excavated by us at the main scarp in order to better document the offset distribution and associated earthquake history.

PT1 was excavated in a scarp segment showing 1.5 to 2 m offsets. During the excavation the trench walls repeatedly collapsed at the position of the fault trace, producing an overhang and a change in orientation of the trench wall. The penultimate event can only indirectly and not unambiguously be recognized by the occurrence of a clay-rich deposit which lacks a counterpart in the hanging wall. We interpret this deposit as the wash part of the colluvial wedge, following the penultimate seismic event and sealing the rupture trace below. This deposit, in turn was cut by faulting during the most recent seismic event. Rupture at this location had occurred along an irregular plane, dipping approximately 40° to the south. The rupture zone is marked by rotated boulders and patches of grus, aligned below large boulders and passively transported along the fault trace. This layer of grus, probably originated from the same clast, has been logged for the length of approximately 1.20 m along the fault trace, corresponding to a vertical offset of about 77 cm.

PT2 reveals a succession of two alluvial deposits (units 1 and 2), covered by an organic-rich soil horizon (unit 3). These three units are faulted by one event. The offset units show a clear drag towards the fault zone. Two parallel associated fault planes dip approximately 36° to the south. The identified paleo-earthquake resulted in a hanging-wall collapse scarp. The associated colluvial wedge, with a maximum thickness of about 65 cm, seals the fault traces. A fine-grained wash deposit covers the wedge and the footwall units. Both, hanging wall and footwall are capped by a thin veneer of recent organic-rich soil. Similar to PT1, granite clasts along the fault lines were cataclasized to grus, which was transported or trapped below larger boulders, but could not attributed to the same source clast and thus did not serve as an offset marker. Furthermore, because the deposits were dragged towards the fault, the offset estimate involves a larger uncertainty. We determined the vertical offset to be approximately 80 cm, based on extrapolation of the contact between units 2 and 3 between meters -1.0 and 1.0 and between meters 3.5 and 5.5, respectively. An offset of 80 cm is in agreement with the vertical offset of the scarp profile, revealed near the trench location (Fig. 2C), resulting in approximately 136 cm of total slip during this event.

Trench PT3, which is located near PT2, but at a higher-offset location associated with a compound scarp segment (2.60 m in the nearest profile, Fig. 2), reveals the evidence for at least two paleo-earthquakes. Unfortunately, the stratigraphic base recording earlier events could not be excavated due to technical limitations. The excavation exposed a southeast-dipping fault zone with two sub-parallel branches. The northern branch ruptured during the penultimate, the southern during the ultimate event, respectively. The fault zone cuts two footwall units and an older colluvial wedge. The northern, older rupture trace contains sheared grus. Along this fault line, the lowest exposed footwall unit is vertically offset by approximately 50 cm, which corresponds to total dip-slip of about 89 cm, assuming a 34° dip of the fault. Above that, a colluvial wedge is recognizable by cataclasized clasts. The younger, southern fault trace extends below the large boulders that limit the excavation of the hanging wall. These boulders have no counterpart in the footwall. The fault plane strikes obliquely to the scarp and is traceable for about 1.20 m inside the trench. It cuts the lower colluvial wedge. The upper colluvial wedge comprises toppled boulders, with carbonate coatings, which are not everywhere on undersides. The vertical offset, when measured at the location of the fault, is on the order of 50 cm, resulting in approximately 76 cm of dip-slip along a 41° dipping fault. However, this is probably underestimated because the offset hanging-wall unit was clearly dragged towards the fault. If measuring the base between meters 6.0 and 7.0, however, which is parallel to the top of the unit and rather horizontal, the vertical offset amounts to approximately 90 cm, or about 1.37 m dip-slip, comparable to the slip observed in PT1 and PT2 for the ultimate event.

Discussion and Conclusion

In all investigated trenches, dip-slip motion was the dominant faulting process, resulting in hanging-wall collapse scarps and the deposition of colluvial wedges. However, the meter-size boulders in the hanging wall of PT3 which abut against the fault trace and which lack a counterpart in the footwall could either reflect a much higher dip-slip offset (i.e., buried boulders) or a lateral component of slip. Overall, we find that the observed offset distribution along the scarp reflects the interplay between surface faulting and alluvial fan dynamics. We find one event in the low-offset segment, which corresponds to alluvial deposits, apparently only marginally incised by ephemeral streams. The other two trenches, which correspond to alluvial-fan lobes that are more dissected and thus possibly more mature, reveal evidence for at least two rupture events, respectively. Unfortunately, the stratigraphic base to further decipher earlier events could not be excavated due to technical issues. Nevertheless, the scarp profile and trenching data show that this area has been repeatedly affected by surface rupturing events, when the fans were active. Preliminary ^{10}Be-surface exposure ages indicate that the faulted alluvial fan must have been active since late

Pleistocene time. The different fan lobes, however, could not be further temporally distinguished. Ongoing age determination of offset strata and colluvial wedges are expected to provide additional data to unravel the faulting history. Besides reported Quaternary activity along the mountain-bounding Chonkurchak fault, the Panfilovkoe scarps indicate ongoing propagation of faulting into the foreland. If this activity, however, superseded activity along the mountain front or if both branches compete in a partitioning of slip, is not yet known. Nevertheless, our new trenching data suggest that the ultimate event recorded in all three trenches was characterized by an offset between 1.2 and 1.4 m, thus recording a major earthquake. Using probabilistic magnitude estimates (after Biasi and Weldon, 2006), this may correspond to a magnitude between 6.8 and 7.2, emphasizing the seismic activity of the northern Tien Shan with infrequent, large magnitude earthquakes.

Acknowledgements: This work was partially supported by the initiative Potsdam Research Cluster for Georisk Analysis, Environmental Change and Sustainability (PROGRESS) and the initiative TIPTIMON (support code 03G0809), by the German Federal Ministry of Education and Research.

References

Abdrakhmatov, K.E., Delvaux, D., & Djanuzakov, K.D., 2002. Active tectonics and seismic hazard of the Issyk-Kul Basin in the Kyrgyz Tian-Shan, in Klerx, J., and Imanackunov, B., eds., *Lake Issyk-Kul: Its natural environment*, Vol. IV. Earth and Environmental Sciences, v. 13, 147-160.

Biasi, G.P. & Weldon II, R.J., 2006. Estimating Surface Rupture Length and Magnitude of Paleoearthquakes from Point Measurements of Rupture Displacement, *Bulletin Seism. Soc. America*, 96(5), 1612-1623.

Eberhart-Phillips, D., Haeussler, P.J., Freymueller, J.T., Frankel, A.D., Rubin, C.M., Craw, P., Ratchkovski, N.A., Anderson, G., Carver, G.A., Crone, J.A., Dawson, T.E., Fletcher, H., Hansen, R., Harp, E.L., Harris, R.A., Hill, D.P., Hreinsdottir, S., Jibson, R.W., Jones, L.M., Kayen, R., Keefer, D.K., Larsen, C.F., Moran, S.C., Personius, S.F., Plafker, G., Sherrod, B., Sieh, K., Sitar, N. & Wallace, W.K., 2003. The 2002 Denali Fault Earthquake, Alaska: A large magnitude, slip-partitioned event, *Science*, 300, 1113-1118.

Hubert-Ferrari, A., Barka, A., Jaques, E., Nalbant, S., Meyer, B., Armijo, R., Tapponier, P. & King, G.C.P., 2000. Seismic hazard in the Marmara Sea region following the 17 August 1999 Izmit earthquake, *Nature,* 404, 269-273.

Kalmetieva, Z.A., Mikolaichuk, A.V., Moldobekov, B.D., Meleshko, A.V., Jantaev, M.M., & Zubovich, A.V., 2009. Atlas of Earthquakes in Kyrgyzstan, ECHO, UNISDR, and CAIAG, pg. 233.

Korjenkov, A., Baipakov, K., Chang, C., Peshkov, Y., & Savelieva, T., 2003. Traces of Ancient Earthquakes in Medieval Cities Along the Silk Road, Northern Tien Shan and Dzhungaria, *Turkish J. Earth Sci*., 12, 241-261.

Rockwell, T.K., Lindvall, S., Herzberg, D., Murbach, D., Dawson, T. & G. Berger, 2000. Paleoseismology of the Johnson Valley, Kickapoo, and Homestead Valley faults: clustering of earthquakes in the eastern California shear zone, *Bulletin Seism. Soc. America*, 90, 1200-1236.

Scholz, Ch.H., 2010. Large Earthquake Triggering, Clustering, and the Synchronization of Faults, *Bulletin Seism. Soc. America*, 100(3), 901-909.

Stein, R.S., Barka, A.A., and Dieterich, J.H., 1997. Progressive failure on the North Anatolian fault since 1939 by earthquake stress triggering*, Geophys. J. Int*.,128, 594-604.

Thompson, S.C., Weldon, R.J., Rubin, C.M., Abdrakhmatov, K., Molnar, P., & Berger, G.W., 2002. Late Quaternary slip rates across the central Tien Shan, Kyrgyzstan, Central Asia, *J. Geophys. Research*, 107

Zubovich, A.V., Wang, X.q., Scherba, Y.G., Schelochkov, G.G., Reilinger, R., Reigber, C., Mosienko, O.I., Molnar, P., Michajljow, W., Makarov, V.I., Li, J., Kuzikov, S.I., Herring, T.A., Hamburger, M.W., Hager, B.H., Dang, Y.m., Bragin, V.D., & Beisenbaev, R.T., 2010. GPS velocity field for the Tien Shan and surrounding regions, *Tectonics*, 29, p. 23, TC6014

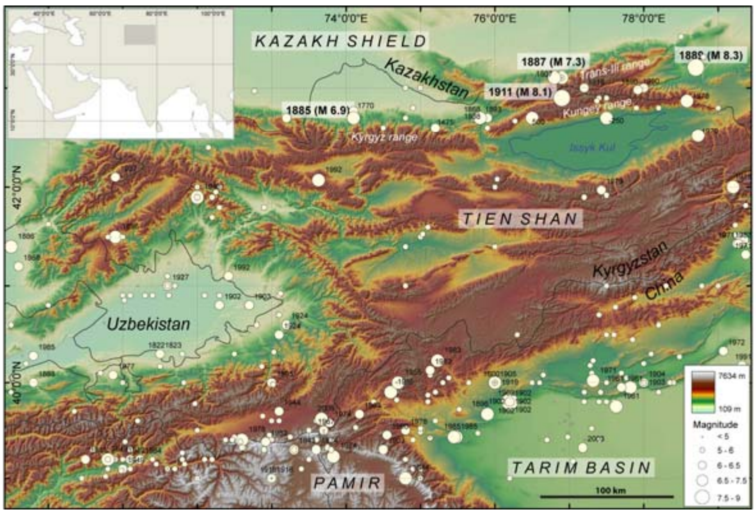

Figure 1: Digital Elevation model (SRTM) of Kyrgyzstan and bordering countries. Major geographic features are labeled. Overlain are historical earthquakes (Kalmetieva et al., 2009), events with magnitudes >6 are labeled with the year of occurrence. Note the series of strong events along the northern rim of the Tien Shan at the turn of the penultimate century. Inset shows position of figure (shaded area) in an Asian-Eurasian framework.

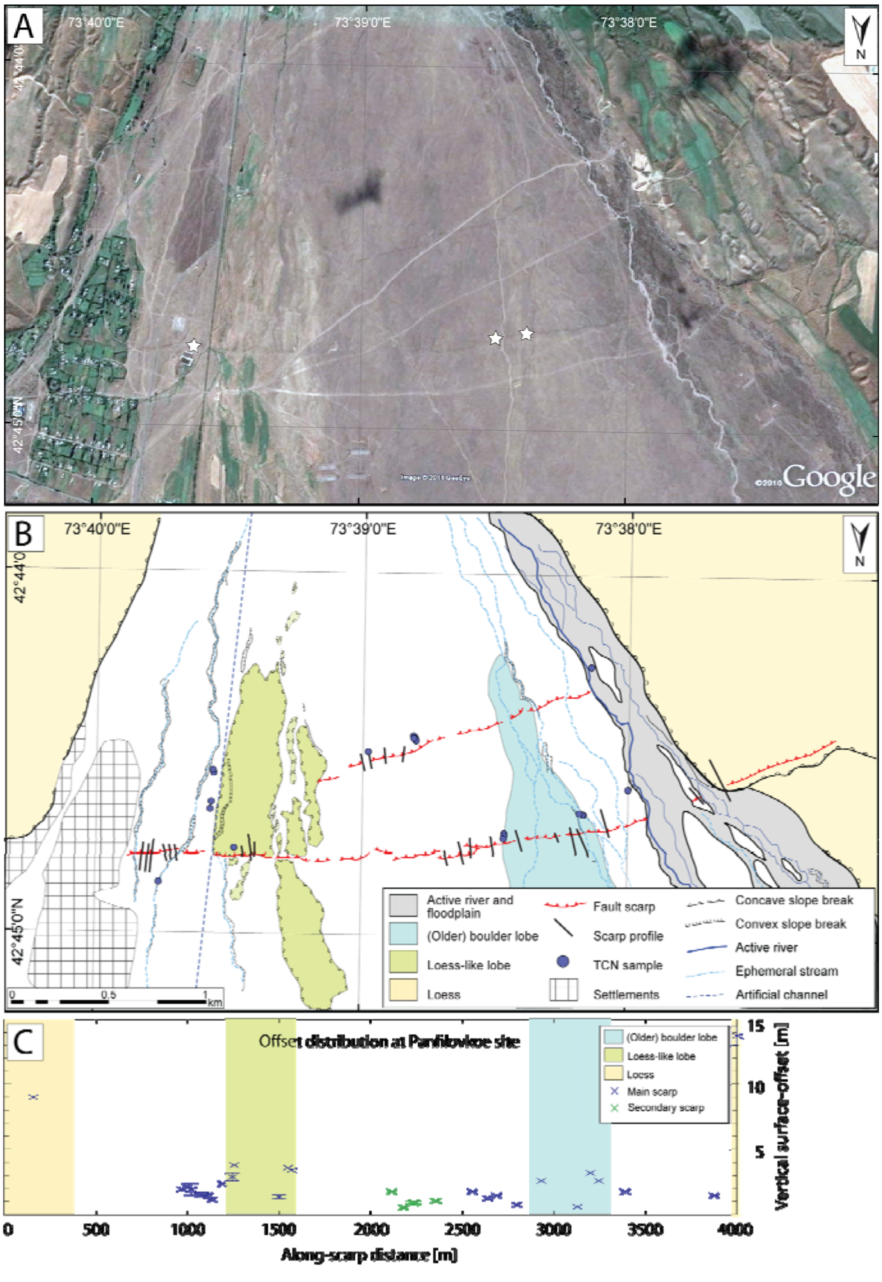

Figure 2: Google Earth satellite image (A) of the Panfilovkoe site showing sub-parallel, linear scarps in the alluvial fan and bordering Loess terrace and the geomorphic interpretation (B). White stars in (A) depict the trench locations (from left to right: PT1, PT2, PT3). Note that the images are rotated. (C) Offset distribution derived from scarp-perpendicular profiles (black lines in (B)).